Supplementary information

Salt-assisted Pyrolysis of Covalent Organic Frameworks into Porous Heteroatom-doped Carbons for Supercapacitive Energy Storage

Dongwan Yan,‡[a] Yang Wu,‡*[a,b] Ryo Kitaura [a] and Kunio Awaga*[a,b]

[a]*Department of Chemistry, Graduate School of Science, Nagoya University, Furo-cho, Chikusa-ku, Nagoya 464-8602, Japan*

[b]*Integrated Research Consortium on Chemical Sciences (IRCCS), Nagoya University, Furo-cho, Chikusa-Ku, Nagoya 464-8602, Japan*

‡These authors contributed equally.

*E-mail: wu.yang@f.mbox.nagoya-u.ac.jp (Y.W.).

*E-mail: awaga.kunio@b.mbox.nagoya-u.ac.jp. (K.A).

1. Materials and Method

All the solvents were purchased from Kanto Chemicals. All chemicals were purchased from TCI. Commercial carbon black VXC72R and Super P were purchased from Tokai carbon and Alfa Aesar, respectively.

1.1 Characterization

Fourier transform infrared (FT-IR) spectra run by a PerkinElmer Spectrum One FT-IR spectrometer using ATR. Scanning electron microscope (SEM) images were obtained on a Hitachi S-4300 field emission SEM. The nitrogen adsorption and desorption isotherms were recorded at 77 K by a BELSOR mini II surface analyser and the specific surface areas were calculated by Brunauer-Emmett-Teller (BET) method. The pore size and pore volume distribution were obtained from the adsorption isotherms by NL-DFT analysis. Powder X-ray diffraction (PXRD) measurement was carried by a Rigaku MultiFlex X-ray diffractometer with the increment of 0.02 ° and diffraction angle range from 1.5 to 60 °. Elemental analysis was recorded on a PerkinElmer 2400 series II CHN elemental analyser. JEOL JEM-2100 plus Field Emission Electron Microscope was used for the high-resolution transmission electron microscopy (HR-TEM) images with the acceleration voltage of 200 kV. High-angle annular dark field (HAADF)-scanning TEM (STEM) was used for the elements mapping at the acceleration voltage of 200 kV. X-ray photoelectron spectroscopy (XPS) data was processed on VG Scientific ESCALab250 with the X-ray source of Al-Kα radiation. Raman spectra were obtained on a HORIBA LabRAM HR-800 excited by 488 nm He-Ne laser with the laser power of 600 μW. Thermal gravimetrical analysis (TGA) plots were obtained on an Exstar TG/DTA 6200 thermal analyser with the ramp up rate of 5 °C min^{-1} using alumina crucibles.

1.2 Electrochemical measurements

1.2.1 Preparation of electrodes for three-electrode system.

The active material slurry was prepared by sonicating of a mixture of active material (NDC-T0, NDC-T1, VXC72R or Super P) (90 wt%) and polyvinylidene fluoride (PVDF) binder (10 wt%) in anhydrous N-Methyl-2-pyrrolidone (NMP) for 1 hour. Then the slurry was coated onto the top of a glassy carbon (GC) electrode with a diameter of 0.5 cm. The active material on the electrode were calculated to be 0.1 mg cm^{-2}.

1.2.2 Electrochemical characterization for three-electrode system.

Electrochemistry plots were conducted on a BioLogic SP-150 single potentiostat electrochemical workstation using a standard three-electrode system in 1M H_2SO_4 aqueous solution. Active material coated glassy carbon electrode was used as a working electrode, Pt wire was used for a counter electrode, and an aqueous Ag/AgCl electrode was used as a reference electrode. The specific capacitances (C_s, F g^{-1}) of the electrodes could be evaluated from the GCD profiles based on the equation, i.e., C_s =

$(I\times\Delta t)/(m\times\Delta V)$, in which, I, Δt, m and ΔV are the discharging current (A), the discharging time (s), the mass of active materials in the electrode (g), and the discharging potential window (V), respectively.

1.2.3 Preparation of electrodes for two-electrode system.

ONC-T1s/CNT hybrid thin films: A mixture of ONC-T1s (10 mg) and CNT (5 mg) were dispersed in DMF (40 ml) using bath sonication for 2 hours. Then, 10 ml of suspension was filtrated through a polytetrafluoroethylene (PTFE) membrane filter (pore size = 0.2 μm, diameter = 25 mm, Merck Millipore) by vacuum filtration. After filtration, the film was washed with ethanol (10 ml) and dried under vacuum for 12h. Then the ONC-T1s/CNT hybrid thin film was peeled off from the filter membrane. The loading weight of ONC-T1s is around 1 mg cm^{-2}.

Pure CNT thin film: 15 mg of CNT was dispersed in DMF (40 ml) using bath sonication for 2 hours. Then, 10 ml of suspension was filtrated through a polytetrafluoroethylene (PTFE) membrane filter (pore size = 0.2 μm, diameter = 25 mm, Merck Millipore) by vacuum filtration. After filtration, the film was washed with ethanol (10 ml) and dried under vacuum for 12h. Then the CNT thin film was peeled off from the filter membrane.

1.2.4 Electrochemical characterization for two-electrode system.

In a two-electrode system, a symmetrical supercapacitor was prepared from two similar-quality electrodes and separated by a filter paper. The electrochemical performance was tested in 1 M H_2SO_4 aqueous solution. The specific capacitance was calculated according to the following equation: $C_s = (2I\times\Delta t)/(m\times\Delta V)$, where C_s (F g^{-1}) is the specific capacitance, I (A) is the discharge current, m (g) is the mass of active material on the one electrode, and ΔV (V) is the potential window.

2. Supplementary Figures

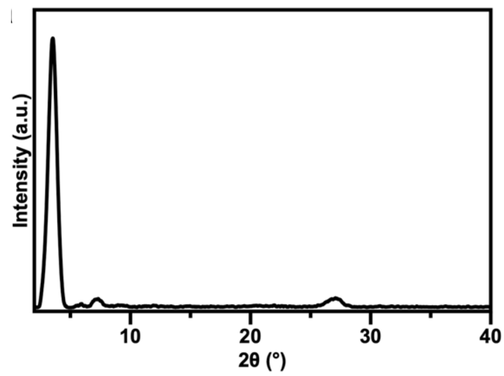

Fig. S1. PXRD pattern of AQ-COF.

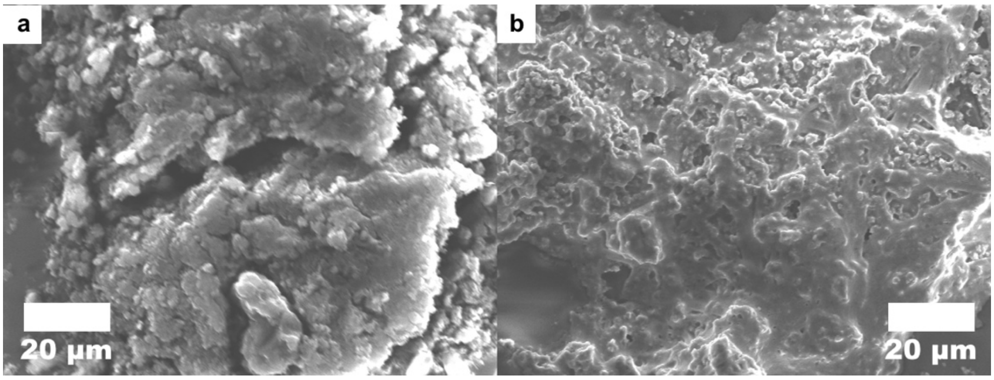

Fig. S2. SEM images of (a) AQ-COF and (b) K_2CO_3@AQ-COF.

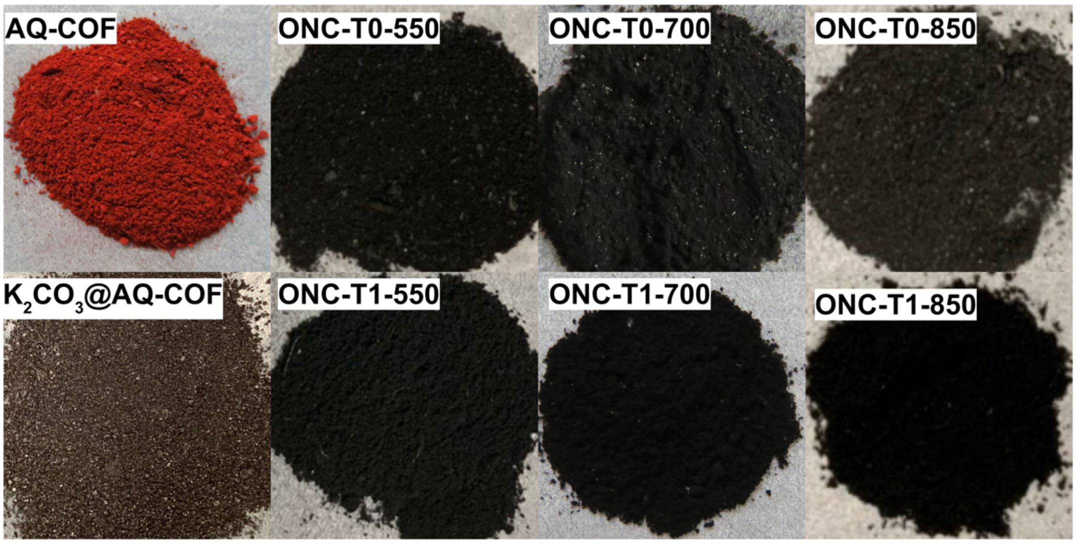

Fig. S3. Photo images of AQ-COF, K_2CO_3@AQ-COF and ONCs.

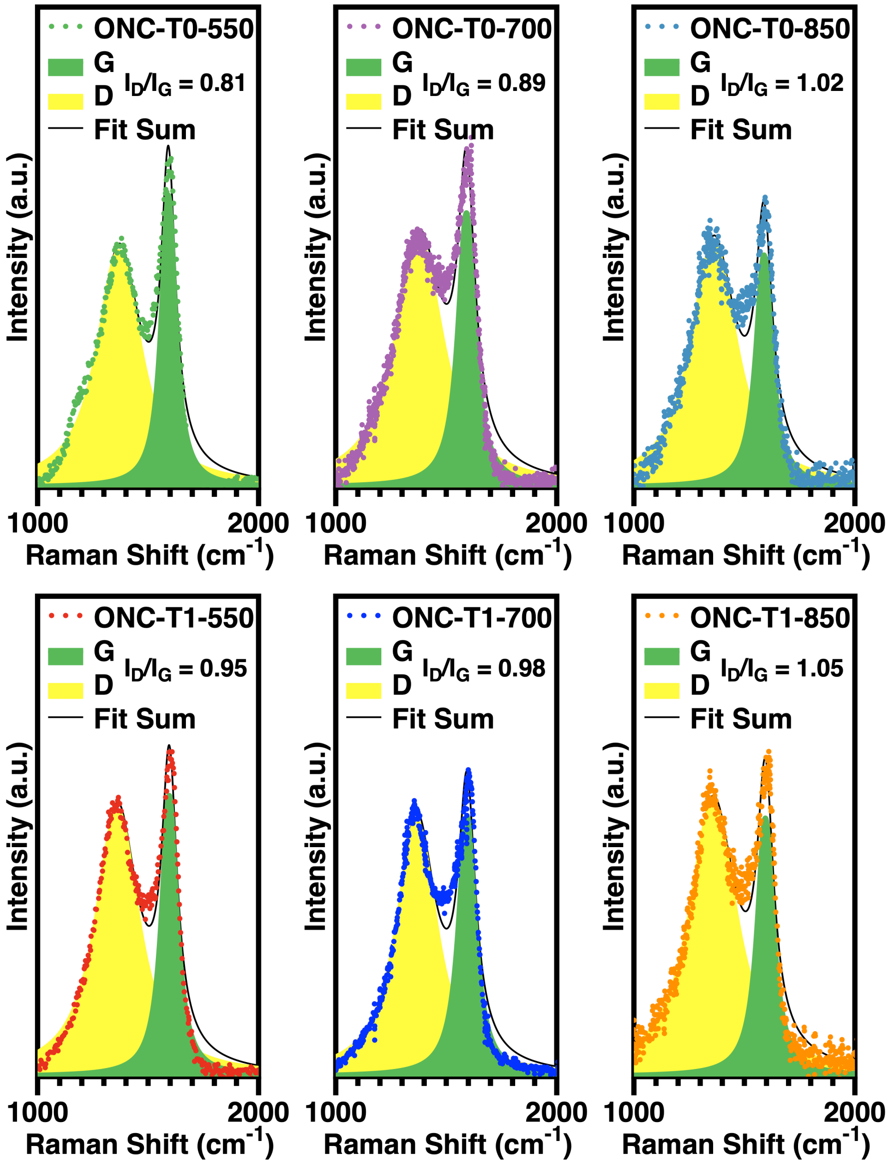

Fig. S4. Raman spectra of ONCs.

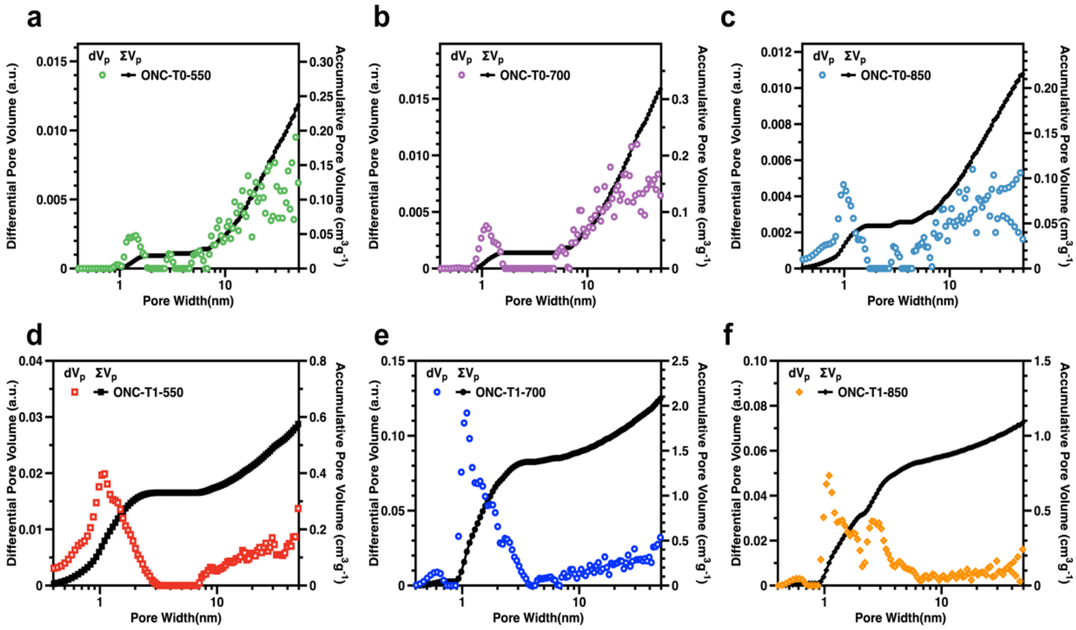

Fig. S5. Pore size and pore volume distribution profiles of ONCs.

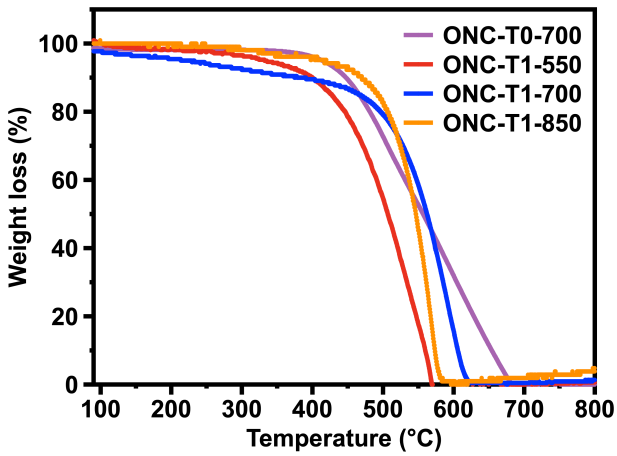

Fig. S6. Analysis of the Thermal Stability of ONCs in air with TGA.

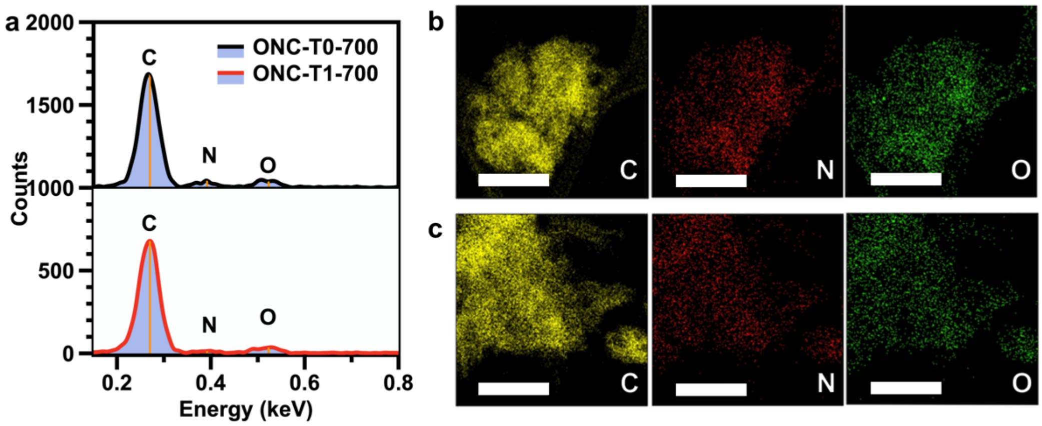

Fig. S7. (a) EDX spectra of ONC-T0-700 and ONC-T1-700. Elemental mapping images of (b) ONC-T0-700 and (c) ONC-T1-700, scale bar = 500 nm.

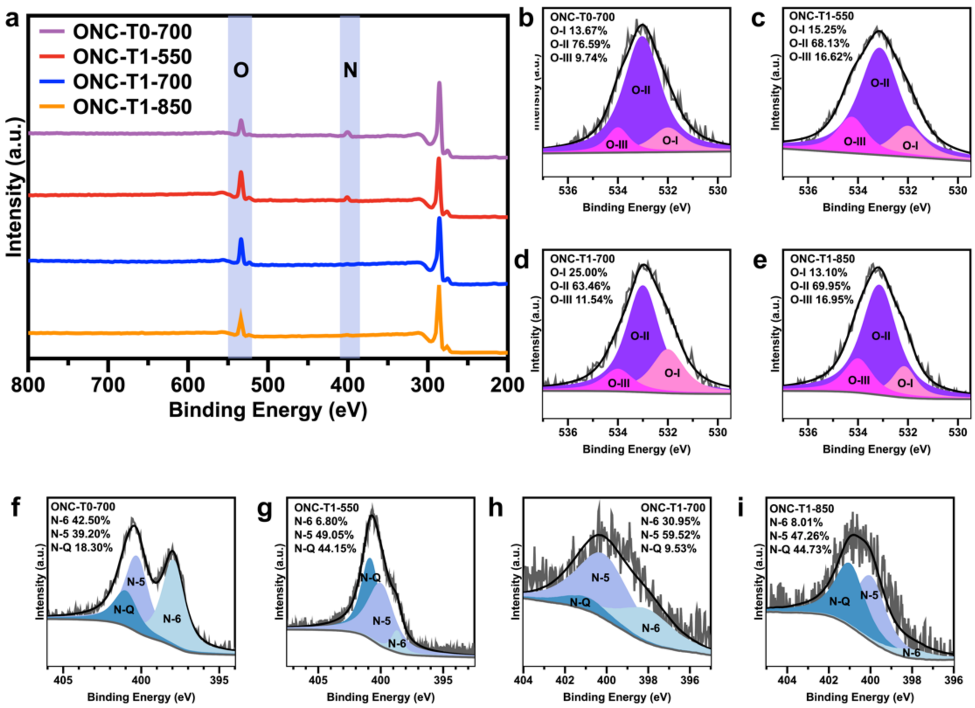

Fig. S8. (a) XPS survey spectra of ONCs. High-resolution XPS spectra of O1s (b-e) and N1s (f-i) in ONCs.

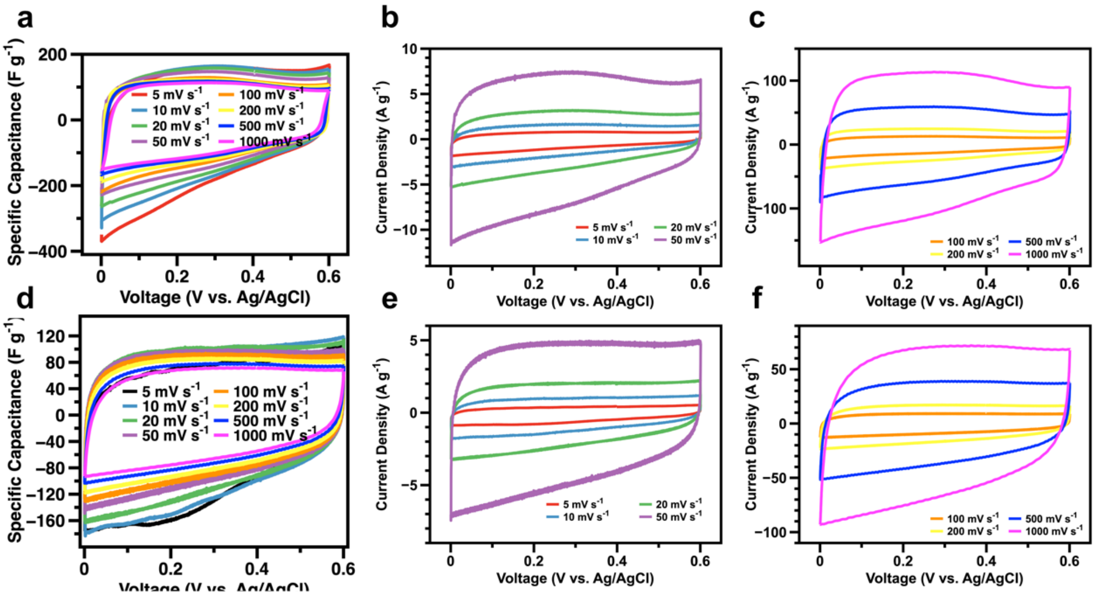

Fig. S9. CV curves of ONC-T0-700 (a-c) and ONC-T0-850 (d-f) recorded at different scan rates.

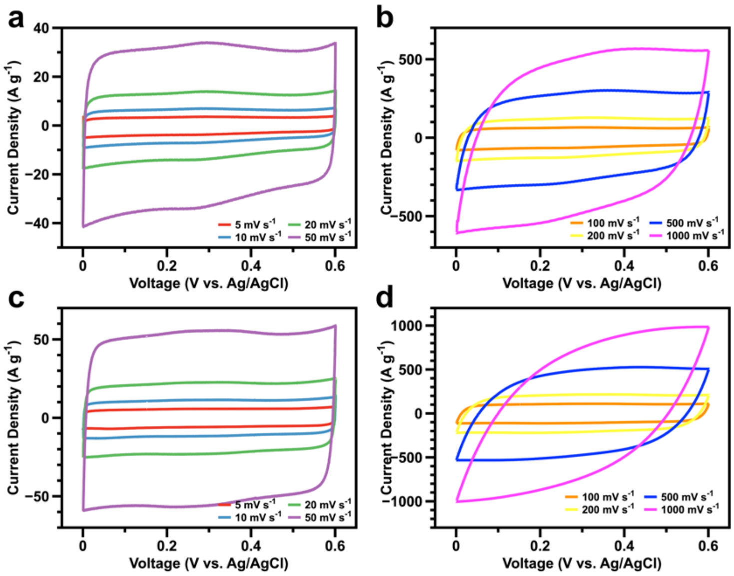

Fig. S10. CV curves of ONC-T1-700 (a and b) and ONC-T1-850 (c and d) recorded at different scan rates.

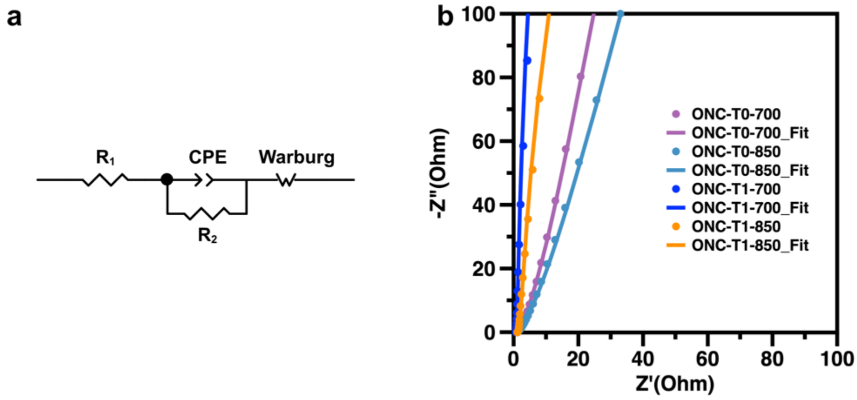

Parameter	ONC-T0-700	ONC-T0-850	ONC-T1-700	ONC-T1-850
Resisitance R_1 [ohm cm^{-2}]	3.68	5.84	3.61	5.81
CPE Y_0 [S s^n cm^{-2}]	0.085	0.016	0.302	0.526
Freq power n	0.94	1	0.92	1
Resisitance R_2 [ohm cm^{-2}]	20,000	39,680	22,205	8,115
Warburg Y_0 [S $s^{0.5}$ cm^{-2}]	0.232	0.085	5.915	2.817

Fig. S11. (a) The equivalent circuit model and (b) the fitting results for EIS of ONC-T0-700, ONC-T0-850, ONC-T1-700 and ONC-T1-850.

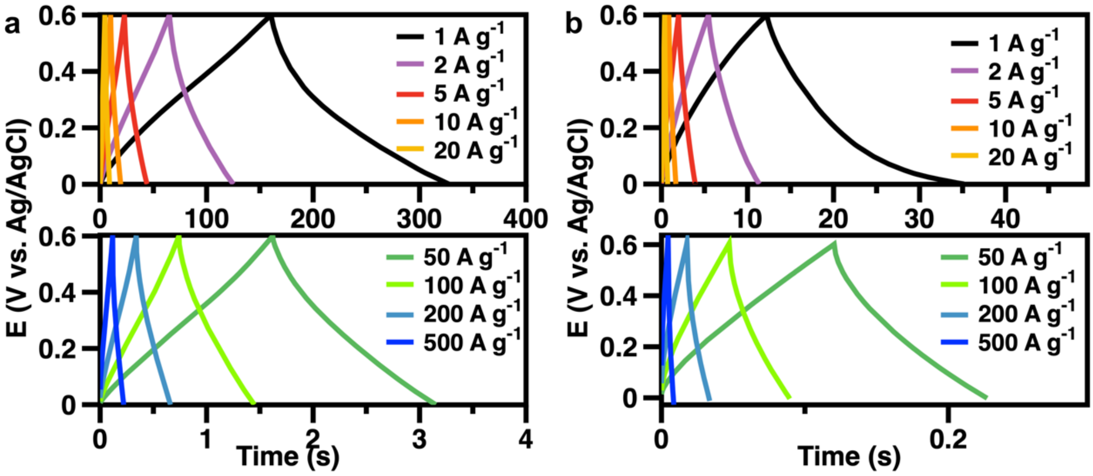

Fig. S12. GCD profiles of ONC-T0-700 (a) and ONC-T0-850 (b) recorded at different current densities.

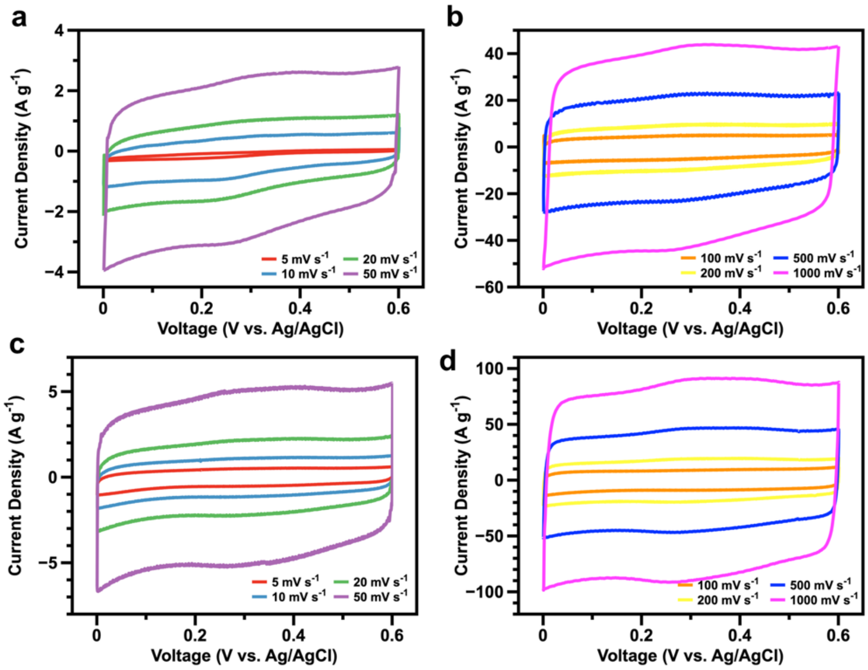

Fig. S13. CV curves of VXC72R (a and b) and Super P (c and d) recorded at different scan rates.

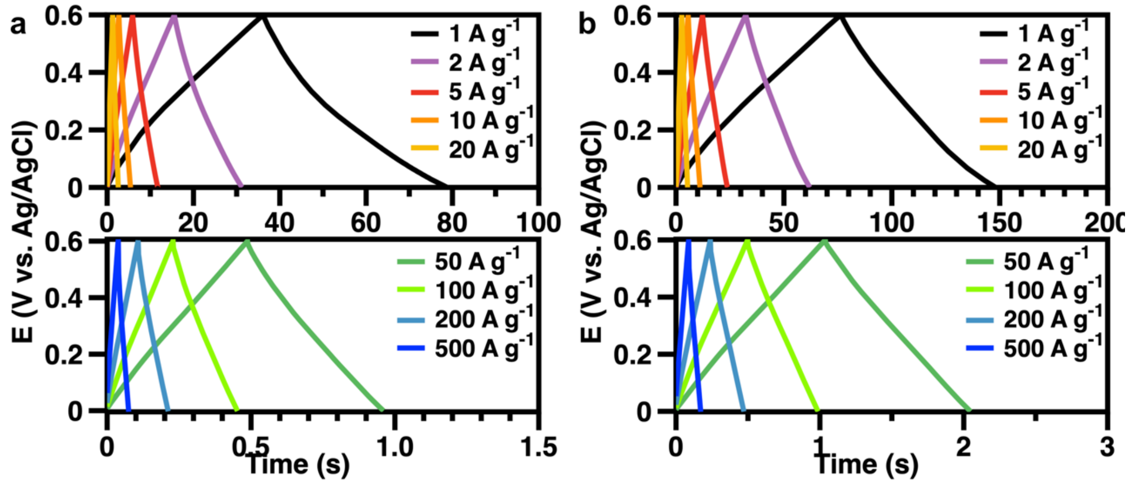

Fig. S14. GCD profiles of VXC72R (a) and Super P (b) recorded at different current densities.

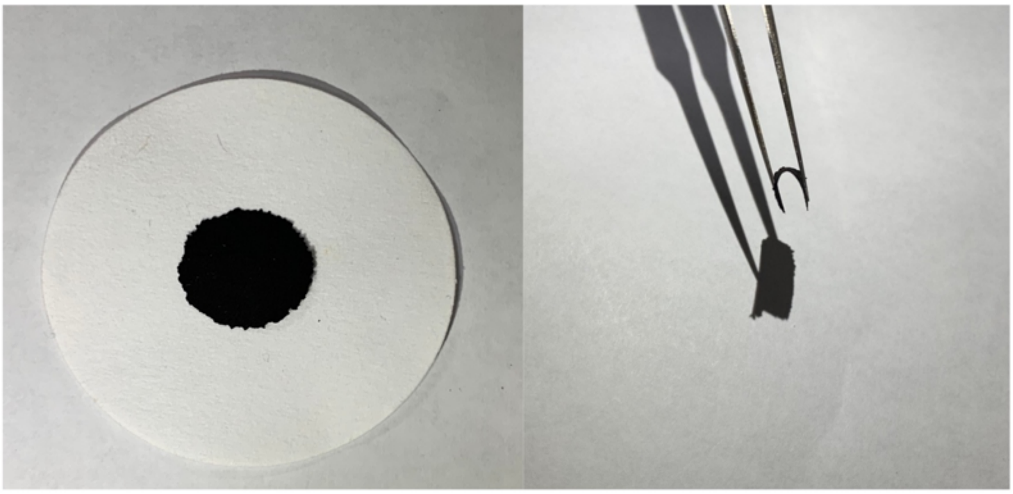

Fig. S15. Photo images of free-standing flexible paper-like ONC-T1s/CNT hybrid thin films.

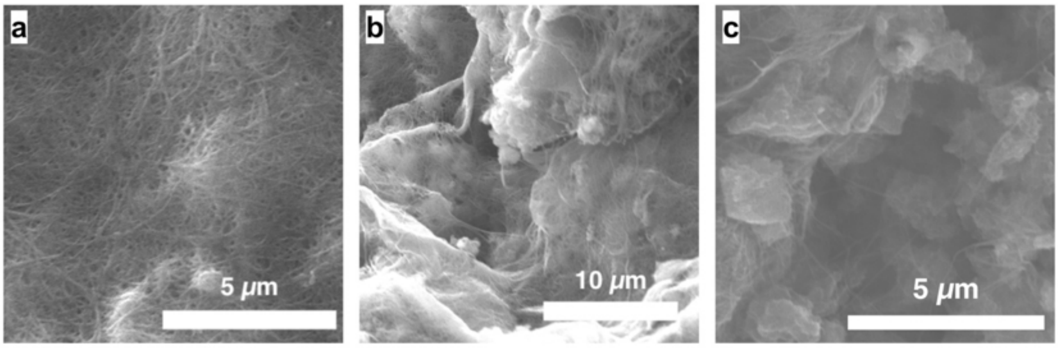

Fig. S16. SEM images of (a) pure CNT film, (b) ONC-T1-700/CNT and (c) ONC-T1-850/CNT hybrid thin films.

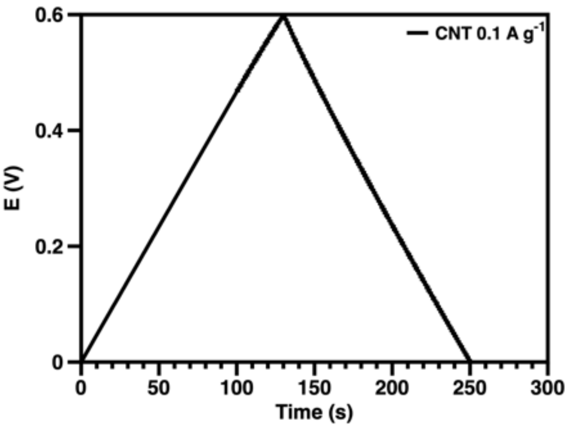

Fig. S17. GCD profile of pure CNT electrodes at a current density of 0.1 A g^{-1} in a two-electrode system.

3. Supplementary Tables

Table S1. Summary of porosity of different COF-derived carbon materials reported to date.

Materials	S_{BET} (m^2 g^{-1})	Pore Volumn (cm^3 g^{-1})	Method	Reference
ONC-T1-700	3451	2.10	K_2CO_3, N_2, 700˚C, 2 h	This work
ONC-T1-850	1518	1.10	K_2CO_3, N_2, 850˚C, 2 h	
ONC-T1-550	823	0.58	K_2CO_3, N_2, 550˚C, 2 h	
ONC-T0-850	157	0.22	N_2, 850˚C, 2 h	
ONC-T0-700	116	0.32	N_2, 700˚C, 2 h	
ONC-T0-550	83	0.24	N_2, 550˚C, 2 h	
BS-COF-C900	720.57	0.39	N_2, 900˚C, 2 h	Adv. Funct. Mater., 2019, 29, 1900161
BS-COF-C700	560.29	0.26	N_2, 700˚C, 2 h	
B-COF-C900	446.2	0.2	N_2, 900˚C, 2 h	
NC-500	87.6	0.27	N_2, 500˚C, 2 h	Appl. Catal. B-Environ., 2019, 244, 25-35
NC-600	74.3	0.22	N_2, 600˚C, 2 h	
NC-700	52.4	0.2	N_2, 700˚C, 2 h	
NC-800	253.6	0.39	N_2, 800˚C, 2 h	
MPC	679	0.476	200˚C,1h anneal, 800˚C,3h	Appl. Surf. Sci., 2018, 439, 833-838
PA@TAPA–DHTA–COF_{1000}	495	0.28	Phytic acid, N_2, 1000˚C, 3 h	Adv. Mater., 2018, 30, 1706330
PA@TAPA–DHTA–$COF_{1000NH3}$	1160	0.59	Phytic acid, N_2, 1000˚C, 3 h; NH_3, 900˚C, 0.5h	
TAPT-$DHTACOF_{0.05}$@$PPZS_{900}$	533	0.25	N_2, 900˚C, 3 h	Chem. Commun., 2017, 53, 11690-11693
TAPT-$DHTACOF_{0.1}$@$PPZS_{900}$	456	0.22		
TAPT-$DHTACOF_{0.2}$@$PPZS_{900}$	421	0.2		
Carbonized ACOF1	1596	1.48	N_2, 800˚C, 10 h	Chem. Eur. J., 2017, 23, 17504-17510
Carbonized COF1	538	0.22		
N(G1)	927	0.959	N_2, 900˚C, 4 h	

N(G2)	1147	0.961	$Fe(acac)_3$, N_2, 900˚C, 4 h	J. Mater. Chem. A, 2017, 5, 4343
N(G3)	844	0.96	$Co(acac)_2$, N_2, 900˚C, 4 h	
N(G4)	893	0.959	$Ni(acac)_2$, N_2, 900˚C, 4 h	
BC-MS-700-3	965	0.8057	3wt % $ZnCl_2$, Ar, 700˚C, 3h	J. Mater. Chem. A, 2016, 4, 4273
BC-MS-700-7	1293	1.5318	7wt % $ZnCl_2$, Ar, 700˚C, 3h	
BC-MS-700-14	1460	1.7678	14wt % $ZnCl_2$, Ar, 700˚C, 3h	
BC-MS-700-21	1329	1.8598	21wt % $ZnCl_2$, Ar, 700˚C, 3h	
BC-MS-900-3	821	-	3wt % $ZnCl_2$, Ar, 900˚C, 3h	
BC-MS-1100	762	-	Ar, 1100˚C, 3h	
NPC700	357	0.43	N_2, 200˚C, 1 h, 700˚C, 3h	ACS Appl. Mater. Interfaces, 2013, 5, 10280-10287
NPC800	525	0.67	N_2, 200˚C, 1 h, 800˚C, 3h	
NPC900	398	0.48	N_2, 200˚C, 1 h, 900˚C, 3h	
POF-C-1000	785	0.701	Furfuryl alcohol, Ar, 1000˚C, 3h,	Chem. Eur. J., 2013,19, 974-980
POF-C-800	335	0.564	Furfuryl alcohol, Ar, 800˚C, 3h,	
POF-DC-1000	100	0.246	Ar, 1000˚C, 3h,	

Table S2. Elemental analysis results of AQ-COF and ONCs.

Samples	Element amount (wt%)			
	C	O	N	H
AQ-COF	66.45	22.02	7.53	4.00
ONC-T0-700	86.58	6.93	6.36	1.13
ONC-T1-550	74.31	16.39	6.11	3.19
ONC-T1-700	93.95	4.55	0.89	0.61
ONC-T1-850	81.81	16.50	1.32	0.37

Table S3. Summary of supercapacitor performance of different carbon-based supercapacitors reported to date. (Sorted by specific capacitance in descending order)

Materials	S_{BET} (m^2 g^{-1})	Specific Capacitance (F g^{-1})	Testing condition	Rate	Electrolyte	Reference
ONC-T1-850	1518	1711	Glassy carbon Three-electrode	1 A g^{-1}	1 M H_2SO_4	This work
OMFLC-N (SM)	-	855	3D-graphene Three-electrode	1 A g^{-1}	0.5M H_2SO_4	Science, 2015, 350, 1508–1513.
ONC-T1-700	3451	768	Glassy carbon Three-electrode	1 A g^{-1}	1 M H_2SO_4	This work
OMFLC-N (S2)	-	730	3D-graphene Three-electrode	1 A g^{-1}	0.5M H_2SO_4	Science, 2015, 350, 1508–1513.
OMFLC-N (S1)	1580	715	3D-graphene Three-electrode	1 A g^{-1}	0.5M H_2SO_4	Science, 2015, 350, 1508–1513.
OMFLC-N (S3)	-	665	3D-graphene Three-electrode	1 A g^{-1}	0.5M H_2SO_4	Science, 2015, 350, 1508–1513.
NG sheets	1555.4	641.6	Nickel foam Three-electrode	1 A g^{-1}	6 M KOH	ACS Appl. Mater. Interfaces, 2014, 6,

						15583-15596
NG hydrogel	297	441	Platinium foil Two-electrode	1 A g^{-1}	1 M H_2SO_4	Adv. Mater., 2013, 25, 5779-5784
NCNFs	2527.7	420	Carbon-coated nickel Two-electrode	5 mV s^{-1}	1 M H_2SO_4	J. Power Sources, 2013, 234, 285-291
HP porous NC spheres	2118	407.9	Nickel foam Three-electrode	1 mV s^{-1}	6 M KOH	Chem. Commun., 2014, 50, 12091-12094
Porous NC spheres	2105.9	398	Glassy carbon Three-electrode	0.2 A g^{-1}	6 M KOH	J. Mater. Chem. A, 2014, 2, 3317-3324
Graphene Quantum Dots	2829	388	Nickel foam Three-electrode	1 A g^{-1}	6 M KOH	J. Mat. Chem. A, 2019, 7, 6021-6027
Porous NCs	3012	385	Nickel foam Two-electrode	0.05 A g^{-1}	6 M KOH	J. Mater. Chem., 2012, 22, 19088-19093
HP NCNTs	3253	365.9	Nickel foam Three-electrode	0.1 A g^{-1}	6 M KOH	J. Mater. Chem. A, 2014, 2, 12545-12551
Porous NCs	1463	363	Titanium mesh Three-electrode	0.1 A g^{-1}	1 M H_2SO_4	Carbon, 2014, 68, 185-194

NG sheets	593	362	Nickel foam Three-electrode	0.2 A g^{-1}	6 M KOH	RSC Adv., 2012, 2, 4498-4506
3D porous NCs	2725	342	Nickel foam Three-electrode	0.2 A g^{-1}	6 M KOH	Nanoscale, 2014, 6, 13831-13837
Porous NCs	2236	341	Nickel foam Two-electrode	0.2 A g^{-1}	6 M KOH	Electrochim. Acta, 2015, 160, 152-159
Porous NC nanoplates	1306	340	Nickel foam Three-electrode	1 A g^{-1}	6 M KOH	Energy Environ. Sci., 2014, 7, 379-386
Porous NCs	645	340	Nickel foam Three-electrode	0.1 A g^{-1}	6 M KOH	Electrochim. Acta, 2015,166, 1-11
Porous NC nanowires	516	327	Nickel foam Three-electrode	0.1 A g^{-1}	6 M KOH	Electrochem. Commun., 2011, 13, 242-246
NG hydrogel	1521	326	Glassy carbon Three-electrode	1 A g^{-1}	6 M KOH	J. Mater. Chem. A, 2013, 1, 2248-2255
Mesoporous NCs	2879	318.2	Nickel foil Three-electrode	0.5 A g^{-1}	6 M KOH	Energy Environ. Sci., 2013, 6, 871-878
Ordered mesoporous NCs	1374	308	Glassy carbon Three-electrode	0.2 A g^{-1}	1 M H_2SO_4	ChemPhysChem, 2014, 15, 2084-2093

Nanoporous carbons NPC-2	803	306	Carbon-cloth Three-electrode	0.5 A g^{-1}	1 M H_2SO_4	Chem. Commun., 2019, 55, 2305-2308
Hollow NC spheres	753	306	Steel mesh Three-electrode	0.1 A g^{-1}	2 M H_2SO_4	J. Mater. Chem., 2012, 22, 13464-13468
Porous NGs/G	1646	300	Nickel foam Three-electrode	0.1 A g^{-1}	6 M KOH	Carbon, 2014, 70, 130-141
NC networks	1724	298	Steel mesh Three-electrode	0.2 A g^{-1}	1 M H_2SO_4	Energy Environ. Sci., 2012, 5, 9747-9751
NG sheets	412.3	295	Nickel foam Three-electrode	5 A g^{-1}	6 M KOH	Carbon, 2014, 69, 66-78
N-doped carbon nanosheets	1169	294	Glassy carbon Three-electrode	0.5 A g^{-1}	6 M KOH	J. Mater. Chem. A, 2015, 3, 13210
Nitrogen- and oxygen-doped carbon	1022	292	Titanium mesh Three-electrode	0.5 A g^{-1}	6 M KOH	RSC. Adv., 2019, 8, 3869-3877
NG sheets	-	282	Nickel foil Two-electrode	1 A g^{-1}	6 M KOH	Nano Lett., 2011, 11, 2472-2477
NG paper	298	280	N-RGO paper Three-electrode	5 mV s^{-1}	1 M H_2SO_4	RSC Adv., 2014, 4, 51878-51883

Porous NCs	2674	280	Titanium mesh Three-electrode	0.2 A g^{-1}	1 M H_2SO_4	Electrochim. Acta, 2015, 158, 229-236
HP NC spheres	568	278	- Three-electrode	0.1 A g^{-1}	1 M H_2SO_4	J. Colloid Interface Sci., 2015, 452, 54-61
Porous NCs/GC	1276	270	Graphite substrate Three-electrode	2 A g^{-1}	1 M H_2SO_4	J. Am. Chem. Soc., 2015, 137, 1572-1580
NC sheets	549.5	249	Glassy carbon Three-electrode	1 A g^{-1}	6 M KOH	J. Mater. Chem. A, 2014, 2, 17297-17301
Actived glucose-derived carbon/CNT hybrids	2021	239	Stainless steel mesh Two-electrode	0.2 A g^{-1}	1 M H_2SO_4	ACS Appl. Mater. Interfaces, 2019, 11, 6066-6077
HP NCs	553	239	Carbon paper Two-electrode	0.5 A g^{-1}	1 M H_2SO_4	ACS Appl. Mater. Interfaces, 2014, 6, 7214-7222
Porous NCs	514	235	Nickel foil Two-electrode	1 A g^{-1}	6 M KOH	J. Power Sources, 2010, 195, 1516-1521
Microporous nitrogen-doped carbon ACOF1	1596	234	Glassy carbon Three-electrode	1 A g^{-1}	6 M KOH	Chem. Eur. J., 2017, 23, 17504-17510
Hollow NC shells	525	230	Nickel net Three-electrode	0.5 A g^{-1}	5 M KOH	ACS Appl. Mater. Interfaces, 2013, 5,

						10280-10287
Porous NC spheres	403	228	Nickel foam Three-electrode	1 A g^{-1}	6 M KOH	Electrochim. Acta, 2015, 158, 166-174
NC film	2870	224.5	Glassy carbon Three-electrode	0.2 A g^{-1}	6 M KOH	Adv. Energy Mater., 2012, 2, 431-437
Ordered mesoporous NCs	320	216	Titanium mesh Three-electrode	0.1 A g^{-1}	1 M H_2SO_4	Electrochim. Acta, 2014, 148, 187-194
Crumpled NGs sheets	465	208	Stainless mesh Two-electrode	0.1 A g^{-1}	1 M H_2SO_4	Langmuir, 2014, 30, 9183-9189
NCNFs-900	562.5	202	Nickel foam Three-electrode	1 A g^{-1}	6 M KOH	Acs Nano, 2012, 6,7092-7102
Ordered mesoporous NCs	761	200	Nickel foam Three-electrode	1 A g^{-1}	6 M KOH	Chem. Mater., 2014, 26, 6872-6877
NG sheets	-	194	Glassy carbon Three-electrode	5 mV s^{-1}	1 M KCl	J. Mater. Chem. A, 2013, 1, 2904-2912
NG hydrogel	-	190.1	Platinum foil Two-electrode	10 A g^{-1}	5 M KOH	Nano Energy, 2013, 2, 249-256
NC porous spheres	475.4	176	Glassy carbon	1 A g^{-1}	1 M H_2SO_4	Polymer, 2014, 55, 2817-2824

			Three-electrode			
Porous NCs	2570	176	Stainless mesh Two-electrode	0.1 A g^{-1}	1 M H_2SO_4	J. Am. Chem. Soc., 2012, 134, 14846-14857
NG sheets	-	170.1	Nickel foam Two-electrode	0.5 A g^{-1}	5 M KOH	Carbon, 2013, 56, 218-223
NG sheets	-	161	Nickel foam Three-electrode	0.5 A g^{-1}	6 M KOH	Electrochim. Acta, 2012, 85, 459-466
NG sheets	-	109.9	Nickel foam Three-electrode	1 A g^{-1}	6 M KOH	Appl. Surf. Sci., 2012, 258, 3438-3443
N, O, P ternary doped porous carbon material	359.67	93.5	Nickel foam Two-electrode	0.1 A g^{-1}	2 M KOH	Chem. Commun., 2019, 55, 1486-1489

Table S4. The properties of ONC-T0-700, ONC-T0-850, ONC-T1-700, ONC-T1-850, VXC72R and Super P.

Materials	S_{BET} (m^2 g^{-1})	V_p (cm^3 g^{-1})			Specific capacitance (F g^{-1})	
		Total	Micro-	Meso-	at 1 A g^{-1}	at 500 A g^{-1}
ONC-T0-700	116	0.32	0.03	0.29	279	86
ONC-T0-850	157	0.22	0.05	0.17	38	3.5
ONC-T1-700	3451	2.10	1.13	0.97	768	439
ONC-T1-850	1518	1.10	0.46	0.64	1711	856
VXC72R	223	0.43	0.11	0.32	71	30
Super P	50.5	0.14	0.02	0.12	119	69